Functional characterization of PCFT/HCP1 as the molecular entity of the carrier-mediated intestinal folate transport system in the rat model

Katsuhisa Inoue,[1] **Yasuhiro Nakai,**[1] **Sayaka Ueda,**[1] **Shunsuke Kamigaso,**[1] **Kin-ya Ohta,**[1] **Mai Hatakeyama,**[2] **Yayoi Hayashi,**[2] **Masaki Otagiri,**[3] **and Hiroaki Yuasa**[1]

[1]*Department of Biopharmaceutics, Graduate School of Pharmaceutical Sciences, Nagoya City University, Nagoya;*
[2]*Department of Biopharmaceutics, College of Pharmacy, Kinjo Gakuin University, Nagoya; and* [3]*Department of Biopharmaceutics, Graduate School of Pharmaceutical Sciences, Kumamoto University, Kumamoto, Japan*

Inoue K, Nakai Y, Ueda S, Kamigaso S, Ohta K, Hatakeyama M, Hayashi Y, Otagiri M, Yuasa H. Functional characterization of PCFT/HCP1 as the molecular entity of the carrier-mediated intestinal folate transport system in the rat model. *Am J Physiol Gastrointest Liver Physiol* 294: G660–G668, 2008. First published January 3, 2008; doi:10.1152/ajpgi.00309.2007.—Proton-coupled folate transporter/heme carrier protein 1 (PCFT/HCP1) has recently been identified as a transporter that mediates the translocation of folates across the cellular membrane by a proton-coupled mechanism and suggested to be the possible molecular entity of the carrier-mediated intestinal folate transport system. To further clarify its role in intestinal folate transport, we examined the functional characteristics of rat PCFT/HCP1 (rPCFT/HCP1) expressed in *Xenopus laevis* oocytes and compared with those of the carrier-mediated folate transport system in the rat small intestine evaluated by using the everted tissue sacs. rPCFT/HCP1 was demonstrated to transport folate and methotrexate more efficiently at lower acidic pH and, as evaluated at pH 5.5, with smaller Michaelis constant (K_m) for the former (2.4 μM) than for the latter (5.7 μM), indicating its characteristic as a proton-coupled folate transporter that favors folate than methotrexate as substrate. rPCFT/HCP1-mediated folate transport was found to be inhibited by several but limited anionic compounds, such as sulfobromophthalein and sulfasalazine. All these characteristics of rPCFT/HCP1 were in agreement with those of carrier-mediated intestinal folate transport system, of which the K_m values were 1.2 and 5.8 μM for folate and methotrexate, respectively, in the rat small intestine. Furthermore, the distribution profile of the folate transport system activity along the intestinal tract was in agreement with that of rPCFT/HCP1 mRNA. This study is the first to clone rPCFT/HCP1, and we successfully provided several lines of evidence that indicate its role as the molecular entity of the intestinal folate transport system.

methotrexate; proton-coupled folate transporter; heme carrier protein; everted sac; oocyte expression system

IT HAS BEEN KNOWN THAT FOLATE (vitamin B9) is absorbed by a specific carrier-mediated transport system from the small intestine (32, 33). The mechanism and regulation of the folate transport system had been of great interest because mammals require the ingestion of preformed folate to meet their needs for one-carbon moieties to sustain key biosynthetic reactions. The folate transport system is also of interest for its role in drug absorption and possible utilization for drug delivery, since it can also mediate the transport of some folate analogs, such as methotrexate, an anticancer and antirheumatic drug.

Reduced folate carrier 1 (RFC1, SLC19A1), which was cloned in 1994 (6, 39), had long been under investigation as a possible molecular entity of the carrier-mediated intestinal folate transport system (2, 22, 26). However, RFC1-mediated transport has been characterized to be optimal at near-neutral pH, whereas the intestinal folate transport system is known to operate optimally at acidic pH. It is also known that RFC1 prefers reduced folates, as its name stands for, to folate as substrates, whereas the intestinal folate transport system prefers folate. Therefore, there had been an argument that some other transporter might be involved in intestinal folate transport. Indeed, proton-coupled folate transporter/heme carrier protein 1 (PCFT/HCP1, SLC46A1) has recently been identified as another folate transporter (19, 23). Although this transporter was originally isolated from the mouse duodenum as a heme transporter (30) and, hence, designated as HCP1 (heme carrier protein 1) at that time, its human ortholog was later found to be able to transport folate more efficiently than heme and its analogs (19, 23). Importantly, PCFT/HCP1 transports folate with affinities comparable with or higher than reduced folates by a proton-coupled mechanism, in agreement with the characteristic of the intestinal folate transport system (27, 28). Thus it is likely that PCFT/HCP1, but not RFC1, is the major molecular entity of the intestinal folate transport system.

We used the rat model in the present study to further clarify the role of PCFT/HCP1 in intestinal folate transport by accomplishing detailed comparison between the folate transport system in the small intestine and PCFT/HCP1. The intestinal folate transport system and rat PCFT/HCP1 (rPCFT/HCP1) were functionally characterized by using everted tissue sacs and *Xenopus laevis* oocytes expression system, respectively, and the distributions of the transport system activity and rPCFT/HCP1 transcript were also examined along the intestinal tract in a comparative manner.

MATERIALS AND METHODS

Chemicals. [3H]folate (1,295 GBq/mmol) and [3H]methotrexate (1,731.6 GBq/mmol) were obtained from Moravek Biochemicals (Brea, CA), and [1,2-14C]polyethylene glycol (PEG) 4000 (0.0333 GBq/g) was from American Radiolabeled Chemicals (St. Louis, MO). Unlabeled folate and methotrexate were obtained from Sigma-Aldrich (St. Louis, MO). Soluene-350, a tissue solubilizer, and Clear-sol II, a scintillation fluid, were obtained from Packard Instrument (Meriden, CT) and Nacalai Tesque (Kyoto, Japan), respectively. All other reagents were of analytical grade and commercially obtained.

Address for reprint requests and other correspondence: H. Yuasa, Dept. of Biopharmaceutics, Graduate School of Pharmaceutical Sciences, Nagoya City Univ., 3-1 Tanabe-dori, Mizuho-ku, Nagoya 467-8603, Japan (e-mail: yuasa @phar.nagoya-cu.ac.jp).

Uptake experiments in everted intestinal tissue sacs. Uptake experiments were conducted using everted tissue sacs (2 cm in length) prepared from the small intestine of male Wistar rats, weighing ~300 g and not fasted, as previously reported (40–42). The experiments were conducted with the approval of the Animal Experiment Ethics Committee of Nagoya City University Graduate School of Pharmaceutical Sciences. In brief, test solutions were prepared in Krebs-Ringer-bicarbonate buffer (118 mM NaCl, 4.7 mM KCl, 2.5 mM CaCl$_2$, 1.2 mM KH$_2$PO$_4$, 1.2 mM MgSO$_4$, 25 mM NaHCO$_3$) added with 20 mM MES (pH 5.5) and oxygenated with 95% O$_2$-5% CO$_2$ gas. When the effect of pH was examined, 20 mM MES was used for pH 5.5 and below and 20 mM HEPES was used for pH 6.0 and above. To test solutions were added trace amounts of ^{3}H-labeled substrate (folate or methotrexate) and ^{14}C-labeled PEG 4000 as a nonabsorbable marker, and also unlabeled substrate (folate or methotrexate) to adjust the concentration. The everted sacs were preincubated for 5 min in substrate-free solution before the initiation of uptake by incubation of the everted sacs in 20 ml of a test solution at a temperature of 37°C and a shaking rate of 100 strokes/min. In experiments to examine the effect of various compounds, test compounds were added only to the test solution so that they were present only during uptake. Uptake was stopped by rinsing the everted sacs briefly in ice-cold saline. A half of each everted sac was placed in a counting vial and its wet weight was determined. The uptake into the tissue was evaluated by determining the radioactivity after solubilization of the sample, by using 1 ml of Soluene-350 as a tissue solubilizer and 5 ml of Clear-sol II as a scintillation fluid.

The jejunum was used in regular experiments. Experiments were also conducted using serially segmented parts of the small intestine or using the ileum.

Isolation of rPCFT/HCP1 cDNA. A BLAST (Basic Local Alignment Search Tool) search of GenBank database using the amino acid sequence of human PCFT/HCP1 (hPCFT/HCP1) as query identified the cDNA sequence of the rat ortholog of PCFT/HCP1 (accession number, NM_001013969.1). Total RNA was prepared from the rat small intestine by a guanidine isothiocyanate extraction method (3). The cDNA of rPCFT/HCP1 was cloned from the total RNA by reverse transcription and subsequent PCR. In brief, a reverse transcription reaction was carried out using 1 μg of the total RNA, an oligo(dT) primer, and ReverTra Ace (Toyobo, Tokyo, Japan) as a reverse transcriptase. From thus obtained cDNA mixture, the coding region of rPCFT/HCP1 cDNA was amplified by PCR using KOD plus polymerase (Toyobo) and the following primers: forward primer, 5′-GTG TCA GCC CCT CGG TGT TCG-3′; reverse primer, 5′-GAG AGC TTG GCC CGG ATC ACA-3′. PCR was performed using the following conditions: 94°C for 2 min; 33 cycles of *1*) 94°C for 20 s, *2*) 59°C for 20 s, and *3*) 72°C for 1.5 min. The amplified cDNA product was subcloned into pTA vector (Toyobo). The coding sequence of rPCFT/HCP1 was amplified by using a forward primer containing an *Eco*RI restriction site (underlined), 5′-GGA ATT CGC CAT GGA GGG GCG CGT GAG C-3′, and the M13 reverse primer for pTA vector. Then the amplified product was introduced at the *Eco*RI and *Hind*III sites into pGH vector (11). The sequence of the amplified cDNA product was determined with an automated sequencer (ABI PRISM 3100; Applied Biosystems, Foster City, CA) and confirmed to be identical to that in GenBank.

Northern blot analysis. The distribution of the transcripts of rPCFT/HCP1 and rat RFC1 (rRFC1) in the rat intestine was examined by Northern blots of total RNA samples. In brief, 20 μg of total RNA isolated by guanidine isothiocyanate extraction from serially segmented parts of the small intestine and the colon was separated on 1% formaldehyde-agarose gels and transferred to a Hybond-XL nylon membrane (GE Healthcare Bio-Sciences, Piscataway, NJ). The UV cross-linked membrane was then hybridized with rPCFT/HCP1-specific and rRFC1-specific cDNA probes, which were labeled with [α-^{32}P]dCTP by use of a random primer DNA labeling kit (GE Healthcare Bio-Sciences), in PerfectHyb (Toyobo) at high stringency

(68°C). Ribosomal RNA (rRNA) was stained with ethidium bromide and used as a reference. Total RNA from various rat tissues was also processed by the same procedure. The tissues of segmented rat intestine and other organs were freshly isolated from male Wistar rats for the extraction of total RNA.

RT-PCR analysis. Total RNA isolated from various rat tissues was used for cDNA synthesis. PCR reactions for rPCFT/HCP1 and glyceraldehyde-3-phosphate dehydrogenase (GAPDH) as a reference were performed using *Taq* DNA polymerase (New England Biolabs Japan, Tokyo, Japan) and the following primers: forward primer for rPCFT/HCP1, 5′-CCG CCA TCA CCG ATC CAT T-3′; reverse primer for rPCFT/HCP1, 5′-GCT GGT GCA CTG GGC TTT AGG-3′; forward primer for GAPDH, 5′-CCA TCA CCA TCT TCC AGG AG-3′; reverse primer for GAPDH, 5′-CCT GCT TCA CCA CCT TCT TG-3′. PCR conditions were as follows: 94°C for 2 min; 35 cycles (rPCFT/HCP1) or 30 cycles (GAPDH) of *1*) 94°C for 20 s, *2*) 60°C for 20 s, and *3*) 72°C for 40 s.

Expression of rPCFT/HCP1 in Xenopus laevis oocytes. The capped cRNA of rPCFT/HCP1 was synthesized from the pGH vector carrying rPCFT/HCP1 cDNA, using AmpliCap-MAX T7 High Yield Message Maker kit (Epicentre, Madison, WI). Stage V and VI oocytes were isolated from mature female *Xenopus laevis* toads by treatment with 2 mg/ml collagenase A (type II; Sigma-Aldrich) at 19°C for 2 h in ND96 solution (96 mM NaCl, 2 mM KCl, 1.8 mM CaCl$_2$, 1 mM MgCl$_2$, and 5 mM HEPES-Tris, pH 7.4) and then maintained in ND96 solution. The oocytes were microinjected either with the cRNA of rPCFT/HCP1 (8 ng/50 nl) or an equivalent amount of water and maintained at 19°C for 3 days in ND96 solution supplemented with penicillin (100 U/ml) and streptomycin (100 μg/ml).

Uptake experiments in Xenopus laevis oocytes expressing rPCFT/HCP1. Uptake solutions were prepared in a modified ND96 solution (pH 5.5) containing 5 mM MES-Tris instead of 5 mM HEPES-Tris. When the effect of pH was examined, 5 mM MES-Tris was used for pH 5.5 and below and 5 mM HEPES-Tris was used for pH 6.0 and above. In regular uptake assays, oocytes were placed in wells of 24-well plates and washed with substrate-free uptake solution (2.5 ml), and uptake assays were started by adding the uptake solution (0.25 ml) containing ^{3}H-labeled substrate (folate or methotrexate). In regular inhibition experiments, test compounds were added only to the uptake solution. In experiments to examine the effect of *p*-chloromercuribenzene sulfonate (*p*CMBS) and HgCl$_2$, which are thiol-modifying reagents, oocytes were pretreated with them in the modified ND96 solution for 5 min, but they were not added to the uptake solution. All the procedures were conducted at 25°C. Assays were stopped by addition of ice-cold substrate-free uptake solution (2.5 ml), and the oocytes were washed two times with 2.5 ml of the same solution. Each oocyte was placed in a counting vial and solubilized in 0.3 ml of 0.2 M NaOH solution containing 0.5% SDS at room temperature for 1 h, and associated radioactivity was measured by liquid scintillation counting, using 3 ml Clear-sol II as a scintillation fluid, for the evaluation of uptake. Oocytes injected with water were used to determine the basal activity for control.

Data analysis. In studies using everted sacs, the uptake was estimated by subtracting the amount in the fluid adhering to the everted sac and that initially adsorbed to it (or instantaneously bound to the membrane) and was expressed in terms of 100 mg wet tissue weight (wtw). The adherent fluid volume was estimated by dividing the amount of PEG 4000 associated with the everted sac by its concentration in the medium. The amount adsorbed (or bound) was estimated as that associated to the tissue during brief (5 s) incubation in the test solution. The uptake rate (*v*) was calculated by dividing the uptake by time during the initial uptake phase (5 min), where uptake was in proportion to time. The amount initially absorbed to the jejunal everted sac was small, being 1.4 ± 0.2 and 1.5 ± 0.2 μl/100 mg wtw (mean $\pm$ SE, $n = 3$) for folate and methotrexate, respectively, as the values normalized by the concentration in the medium (C$_m$) at the C$_m$

of 10 nM and pH 5.5 as the condition for regular uptake experiments. They were only ~2–3% of uptake at 5 min.

In studies using *Xenopus laevis* oocytes, *v* was calculated by dividing the uptake by time during the initial uptake phase (30 min), where uptake was in proportion to time. For both folate and methotrexate, the amount in the fluid adhering to the oocyte and that initially adsorbed to it were negligible. The rPCFT/HCP1-specific uptake was estimated by subtracting the uptake in water-injected oocytes from that in rPCFT/HCP1-expressing oocytes.

In both types of studies, the uptake clearance (CL_{up}) was calculated by dividing *v* by C_m. The expression of CL_{up} for Michaelis-Menten type carrier-mediated transport is as follows: $CL_{up} = V_{max}/(K_m + C_m)$. The kinetic parameters of maximum transport rate (V_{max}) and the Michaelis constant (K_m) were estimated by fitting this equation to the experimental data of CL_{up} vs. C_m profiles by means of nonlinear least-squares regression analysis using WinNonlin (Pharsight, Mountain View, CA) and the reciprocal of variance as the weight. The parameters are presented as the computer-fitted ones with SE.

Experimental data are presented as means ± SE, and statistical analysis was performed using Student's *t*-test or, when multiple comparisons were needed, ANOVA followed by Dunnett's test, with $P < 0.05$ considered significant.

RESULTS

Functional characteristics of carrier-mediated folate transport system in the jejunum. The uptakes of both folate and methotrexate in the everted tissue sacs of the rat jejunum were in proportion to time at least up to 10 min at their trace concentration of 10 nM in an acidic medium of pH 5.5, as shown in Fig. 1. It was also observed that they were greater at lower pH, being greatest at pH 5.0 to 5.5 and negligibly small at around neutral pH and above, indicating the involvement of highly pH-dependent uptake mechanism that optimally operates at acidic pH (Fig. 2). On the basis of these results, we chose 5-min uptake period and pH 5.5 as the condition in subsequent experiments for both folate and methotrexate to evaluate transport across the cellular membrane in the initial uptake phase and at an highly efficient level.

The jejunal uptakes of both folate and methotrexate were highly saturable, as indicated by a decrease in the uptake clearance with an increase in the concentration (Fig. 3). Both of them conformed to the Michaelis-Menten kinetics without
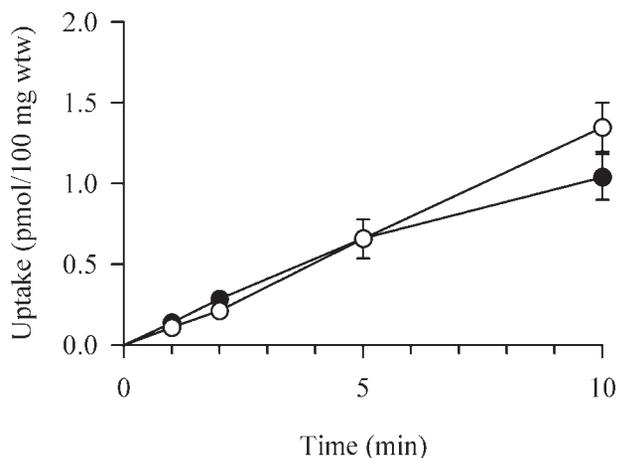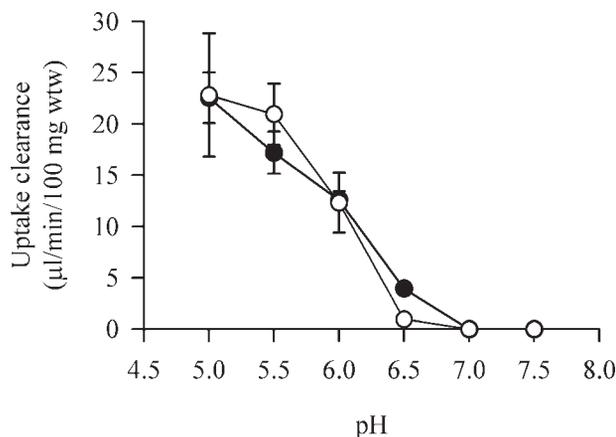
Fig. 2. pH dependence of the uptakes of folate and methotrexate in the everted sacs of the rat jejunum. Data represent means ± SE (*n* = 3). The uptakes of folate (10 nM; ●) and methotrexate (10 nM; ○) were evaluated at 37°C and for 5 min.

nonsaturable transport, indicating that carrier-mediated transport is responsible for the both and that neither of the two compounds is permeable by diffusive transport. Accordingly, the uptake clearances of both compounds were reduced to be negligibly small at the highest concentration of 100 μM. Although the uptakes of the two compounds were comparable at lower concentrations with overlapping pH-dependent uptake profiles shown in Fig. 2, the K_m was about fivefold greater for methotrexate (5.8 μM) than for folate (1.2 μM), and, accordingly, so was the V_{max}. In addition, we also observed that the uptake of folate (10 nM) was completely inhibited to be an undetectable level by 100 μM of methotrexate and so was the uptake of methotrexate (10 nM) by 100 μM of folate (data not shown).

All these results, combined together, indicate that folate and methotrexate share an only carrier-mediated transport system for them in the rat jejunum. The transport system is highly pH dependent with an acidic pH optimal for operation and has a higher affinity for folate than for methotrexate. Thus we could
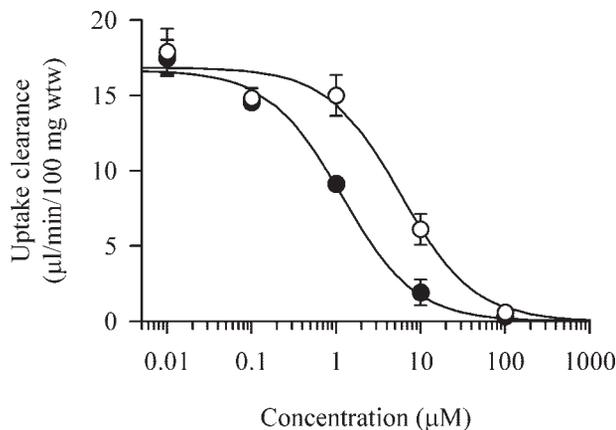
Fig. 1. Time courses of the uptakes of folate and methotrexate in the everted sacs of the rat jejunum. Data represent means ± SE (*n* = 3). The uptakes of folate (10 nM; ●) and methotrexate (10 nM; ○) were evaluated at 37°C and pH 5.5. wtw, Wet tissue weight.

Fig. 3. Concentration dependence of the uptakes of folate and methotrexate in the everted sacs of the rat jejunum. Data represent means ± SE (*n* = 3). The uptakes of folate (●) and methotrexate (○) were evaluated at 37°C and pH 5.5 for 5 min. Solid lines represent the computer-fitted profiles. The values of V_{max} (pmol·min^{-1}·100 mg wtw^{-1}) and K_m (μM) are 19.5 ± 2.9 and 1.2 ± 0.2, respectively, for folate and 98.3 ± 24.6 and 5.8 ± 1.3, respectively, for methotrexate as the computer-fitted parameters with SE.

clearly demonstrate by initial uptake assessments in the jejunal everted sac as the rat tissue model all these important characteristics known for the carrier-mediated intestinal folate transport system, which have been reported in pieces in various intestinal preparations, brush border membrane vesicles (17, 28), everted sacs (34) and sheets (46) of the excised tissue, and the perfused intestine in situ (4, 5, 25).

Effect of various compounds on folate uptake in the jejunum. Chemical structural requirements to be recognized by the carrier-mediated folate transport system were assessed by examining the effect of various compounds on the jejunal uptake of folate at its trace concentration of 10 nM. We first examined the effect of carboxylate-type compounds (Fig. 4). Although folate has a glutarate-like moiety in its molecule, glutarate, an endogenous dicarboxylate, was found not to inhibit folate uptake even at a concentration as high as 5 mM. α-Ketoglutarate, a ketonized endogenous derivative of glutarate, did not, either. Among the others, which are all monocarboxylate-type drugs, diclofenac, indomethacin, and sulfasalazine were found to inhibit folate uptake significantly. Sulfasalazine was the most potent inhibitor. Among some other types of compounds (Fig. 5), sulfobromophthalein (BSP), a sulfate-type compound, was found to inhibit folate uptake extensively. All the other compounds did not affect folate uptake significantly. They include thiamine pyrophosphate (TPP) and thiamine monophosphate (TMP) as inhibitors of RFC1 (44, 45), phenytoin and phenobarbital as weakly acidic non-carboxylate-type drugs, cimetidine as a cationic drug, 5-fluorouracil as a substrate of the carrier-mediated pyrimidine transport system (40), and taurocholate as a substrate of apical sodium-dependent bile acid transporter (ASBT, SLC10A2) (38). Thus having negative charge seems to be required to be recognized by the folate transport system as a substrate or inhibitor. The carboxylate moiety may also play a role in substrate recognition.

It is known that methotrexate is a substrate of breast cancer resistance protein (BCRP, ABCG2) and multidrug resistance-assoc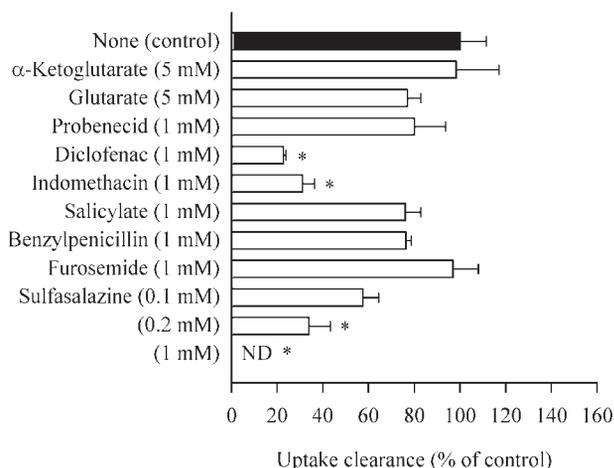iated protein 2 (MRP2, ABCC2), which are secretory transporters suggested to be present in the small intestine (1, 14). Folate has also been suggested to be a substrate of BCRP (1). We therefore also examined the effect of diethylstilbestrol and estrone-3-sulfate, which are inhibitors of BCRP (35) and of BCRP and MRP2 (18), respectively, on the uptakes of methotrexate and also of folate to examine whether the uptake might be modulated by those secretory transporters. However, the jejunal uptake of folate was increased by neither diethylstilbestrol nor estrone-3-sulfate, and so was that of methotrexate (Table 1). In the ileum, the uptakes of both compounds remained undetectable in the presence of these inhibitors as well as in their absence (data not shown). Thus there was no sign of inhibition of secretory transport, indicating the insignificant role of BCRP and MRP2 in the uptakes of both folate and methotrexate.

Structural features of rPCFT/HCP1. The cDNA of rPCFT/HCP1, which was identified by a BLAST search of GenBank database using the amino acid sequence of hPCFT/HCP1, was found to encode a putative protein of 459 amino acids. Hydropathy analyses using a program, SOSUI (http://bp.nuap. nagoya-u.ac.jp/sosui/), predicted 11 potential membrane-span-

Fig. 5. Effect of various compounds on folate uptake in the everted sacs of the rat jejunum. Data represent means ± SE ($n = 3$). The uptake of folate (10 nM) was evaluated at 37°C and pH 5.5 for 5 min in the presence of a test compound (1 mM) or in its absence. The control value was 16.6 μl·min^{-1}·100 mg wtw^{-1}. BSP, bromosulfophthalein; TPP, thiamine pyrophosphate; TMP, thiamine monophosphate. *Significantly different from the control at $P < 0.05$; **test compound dissolved in DMSO (0.5%).

Fig. 4. Effect of carboxylate-type compounds on folate uptake in the everted sacs of the rat jejunum. Data represent means ± SE ($n = 3$). The uptake of folate (10 nM) was evaluated at 37°C and pH 5.5 for 5 min in the presence or absence of a test compound. The control value was 20.1 μl·min^{-1}·100 mg wtw^{-1}. The test compounds were dissolved in DMSO (0.5%) except for salicylate. ND, not detected. *Significantly different from the control at $P < 0.05$.
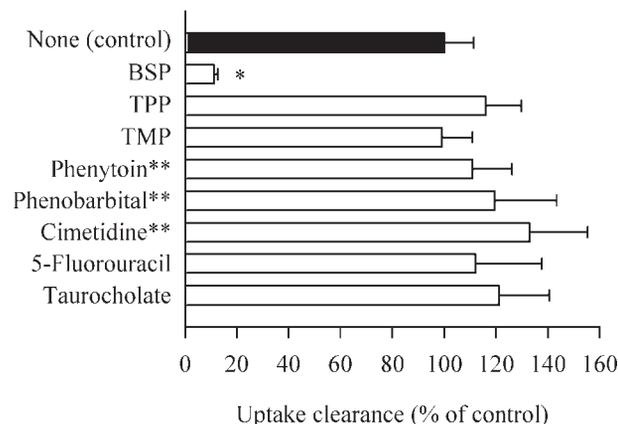
Table 1. *Effect of inhibitors of secretory transporters on the uptakes of folate and methotrexate in the everted sacs of the rat jejunum*

Substrate and Inhibitor	Uptake Clearance, % of control
Folate	
None (control)	100.0±11.5
Diethylstilbestrol (0.02 mM)	115.5±9.9
Estrone-3-sulfate (1 mM)	62.3±15.2
Methotrexate	
None (control)	100.0±26.7
Diethylstilbestrol (0.02 mM)	76.7±15.2
Estrone-3-sulfate (1 mM)	49.4±6.5

Data represent means ± SE ($n = 3$). The uptakes of folate (10 nM) and methotrexate (10 nM) were evaluated at 37°C and pH5.5 for 5 min in the presence or absence of a test compound. The control values for folate and methotrexate were 20.9 and 17.8 μl·min^{-1}·100 mg wet tissue weight^{-1}, respectively.

ning domains. Putative extracellular *N*-glycosylation sites were found at residues of Asn[58] and Asn[68]. rPCFT/HCP1 is 87% identical with and 91% similar to hPCFT/HCP1, which also has 459 amino acids and putative 11 membrane spanning domains.

Distribution of carrier-mediated folate transport system in the small intestine. We then examined the distribution of the activity of the carrier-mediated folate transport system in the small intestine and compared with the distribution of the mRNA of rPCFT/HCP1. As shown in Fig. 6, the uptakes of both folate and methotrexate, which were determined at their trace concentration of 10 nM, were found to be high in the upper half of the small intestine (duodenum and jejunum), decreased downwardly in the subsequent quarter and were undetectably low in the last quarter (the lowest ileum). This observation that the profiles of the uptake along the intestinal tract were overlapped for the two substrates is consistent with the suggestion that they share the same folate transport system. Such distribution profile of the carrier-mediated folate transport system activity was in agreement with that of the mRNA of rPCFT/HCP1 evaluated by Northern blot (Fig. 7), suggesting its role as the molecular entity of the folate transport system. Particularly in the lowest ileum where the mRNA of rPCFT/HCP1 was almost undetectable, so was the folate transport system activity, indicating that rPCFT/HCP1-mediated transport is the only mechanism for the uptakes of folate and methotrexate. This is in agreement with the finding for their jejunal uptakes that nonsaturable (diffusive) transport was kinetically negligible. In contrast to that, the mRNA of rRFC1 was found to be distributed evenly in the entire small intestine. Thus its distribution profile is obviously different from that of the folate transport system activity and, hence, its contribution in the activity is unlikely. It is also notable that rPCFT/HCP1 is expressed almost exclusively in the small intestine, indicating its role as the intestine-specific folate transporter, whereas RFC1 is expressed ubiquitously in various tissues (Fig. 8*A*). Although RT-PCR revealed the expression of rPCFT/HCP1 in many other tissues, with the only exception of skeletal muscle (Fig. 8*B*), its expression in those tissues does not seem to be high enough to be detected by Northern blot. This tissue

Fig. 7. Northern blot analysis for the expression of the mRNAs of rPCFT/HCP1 and rRFC1 in various regions of the rat small intestine. Total RNA from each intestinal region was probed with ^{32}P-labeled cDNA of rPCFT/HCP1 and that of rRFC1. The bands of ethidium bromide-stained rRNA are also shown as references. Numbers represent regions used in the uptake experiments shown in Fig. 4.

distribution profile of rPCFT/HCP1 is different from that of its human counterpart (hPCFT/HCP1), which is reportedly expressed also in kidney, liver, placenta, and spleen at substantial levels and, to lesser extents, in colon and testis (23). There may be some species differences in the tissue distribution of PCFT/HCP1.

Functional characteristics of rPCFT/HCP1 expressed in Xenopus laevis oocytes. We finally examined the transport of folate and methotrexate mediated by rPCFT/HCP1 expressed in *Xenopus laevis* oocytes to identify that it is a folate transporter as its human ortholog. The uptakes of the both compounds at their trace concentration of 10 nM in an acidic medium of pH 5.5 were much greater in oocytes injected with the cRNA of rPCFT/HCP1 than in control oocytes injected
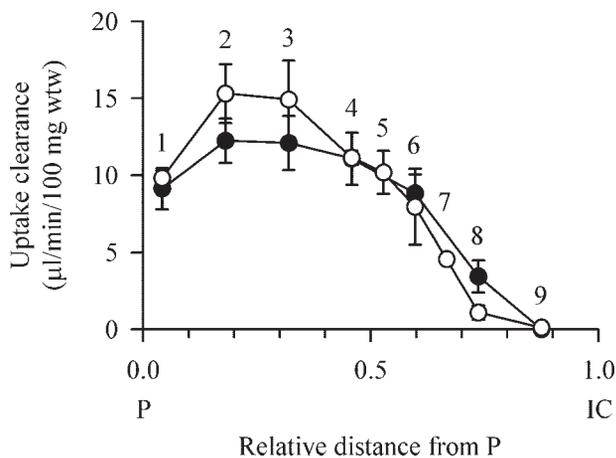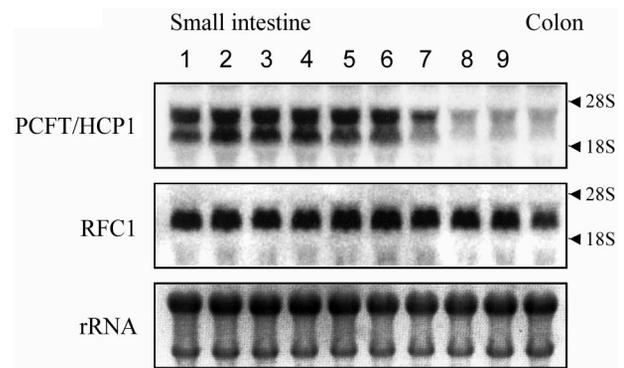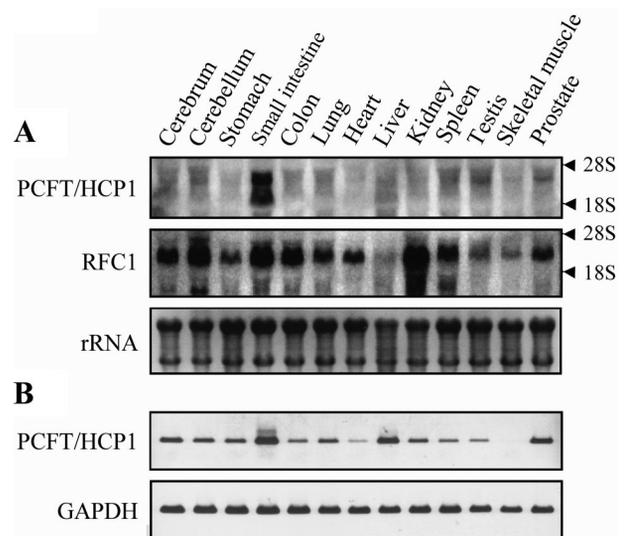

Fig. 6. Uptakes of folate and methotrexate by everted sacs from various regions of the rat small intestine from pylorus (P) to ileocecal junction (IC). Data represent means ± SE (*n* = 6 for folate and 3 for methotrexate). The uptakes of folate (10 nM; ●) and methotrexate (10 nM; ○) were evaluated at 37°C and pH 5.5 for 5 min.

Fig. 8. Northern blot analysis for the expression of the mRNAs of rPCFT/HCP1 and rRFC1 (*A*) and RT-PCR analysis for the expression of the mRNA of rPCFT/HCP1 (*B*) in various tissues of the rat. Total RNA from each tissue was probed with ^{32}P-labeled cDNA of rPCFT/HCP1 and that of rRFC1 in Northern blot analysis. The bands of ethidium bromide-stained rRNA are also shown as references. Total RNA (3 μg) from each tissue was reverse transcribed and then amplified by PCR using a set of specific primers for rPCFT/HCP1 in RT-PCR analysis. The bands of GAPDH are also shown as references.
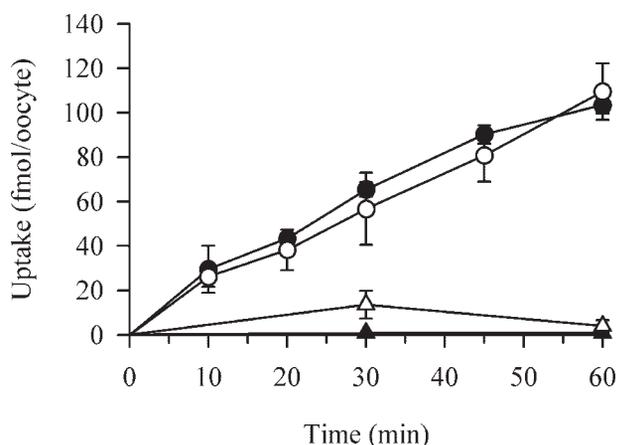
Fig. 9. Time courses of the uptakes of folate and methotrexate in *Xenopus laevis* oocytes expressing rPCFT/HCP1. Data represent means ± SE (*n* = 3). The uptakes of folate (10 nM; ●) and methotrexate (10 nM; ○) were evaluated at 25°C and pH 5.5 in rPCFT/HCP1-expressing oocytes and water-injected control oocytes.

Fig. 11. Concentration dependence of the uptakes of folate and methotrexate mediated by rPCFT/HCP1 expressed in *Xenopus laevis* oocytes. Data represent means ± SE (*n* = 6 or 8). The uptakes of folate (●) and methotrexate (○) were evaluated at 25°C and pH 5.5 for 30 min in rPCFT/HCP1-expressing oocytes and water-injected control oocytes. The rPCFT/HCP1-specific uptake was estimated by subtracting the uptake in the latter from that in the former and was used for kinetic analysis. Solid lines represent the computer-fitted profiles. The values of V_{max} (fmol·min^{-1}·oocyte^{-1}) and K_m (μM) are 0.51 ± 0.06 and 2.4 ± 0.4, respectively, for folate and 1.73 ± 0.17 and 5.7 ± 0.7, respectively, for methotrexate, as the computer-fitted parameters with SE.

with water (Fig. 9), indicating their efficient uptakes by rPCFT/HCP1 expressed from the injected cRNA. The uptakes of both compounds were in proportion to time at least up to 30 min in the rPCFT/HCP1-expressing oocytes, whereas they remained only minimal in the water-injected oocytes. Furthermore, the uptakes in the former were greater at lower pH, being greatest at pH 5.0 to 5.5, and negligibly small at around neutral pH (Fig. 10), demonstrating the characteristic of rPCFT/HCP1 as a proton-coupled transporter, whereas the uptakes in the latter were only minimal and pH-independent. In subsequent experiments, we therefore evaluated the rPCFT/HCP1-mediated uptake by uptake measurements at pH 5.5 in the initial uptake period of 30 min.

The rPCFT/HCP1-mediated uptakes of folate and methotrexate were both saturable, conforming to the Michaelis-Menten kinetics (Fig. 11). The values of K_m, 2.4 μM and 5.7 μM for folate and methotrexate, respectively, were comparable with the respective K_m values for folate (1.2 μM) and methotrexate (5.8 μM) in the everted tissue sacs of the rat jejunum.
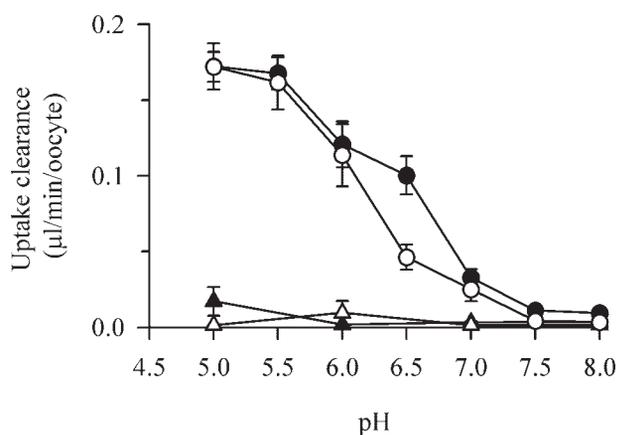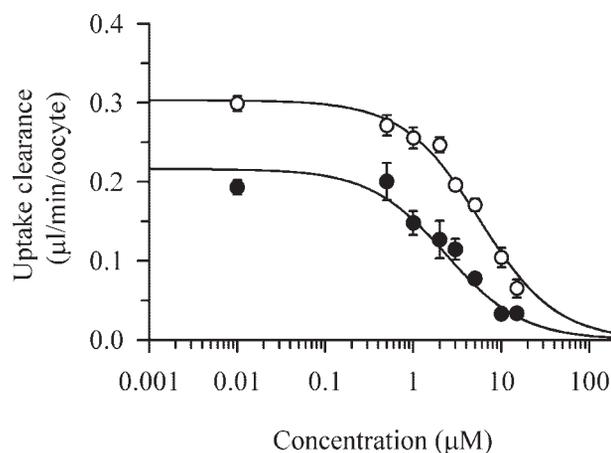
The effect of various compounds on the rPCFT/HCP1-mediated uptake of folate was examined at its trace concentration of 10 nM. It was found that sulfasalazine and BSP, which are potent inhibitors in the everted sacs, inhibit rPCFT/HCP1-mediated folate uptake potently (Fig. 12), and diclofenac and indomethacin, which are less potent inhibitors, do less potently. α-Ketoglutarate, which did not inhibit intestinal folate uptake in everted sacs, was found not to inhibit rPCFT/HCP1-mediated folate uptake, either. Some other compounds that did not show inhibitory effect include lactate, another endogenous carboxylate, L-glutamate, of which folate is a derivative, and TMP as an inhibitor of RFC1, whereas DIDS was additionally found to be a potent inhibitor. Thus the results
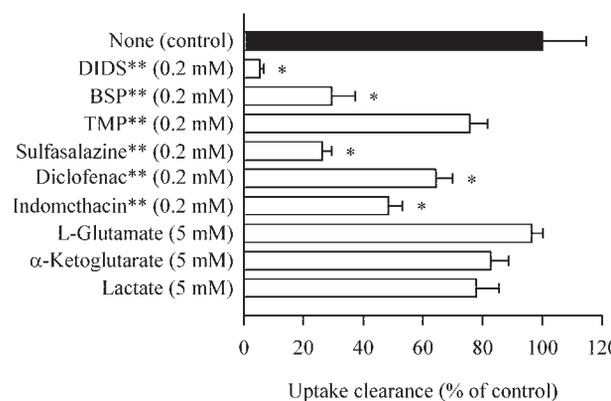

Fig. 10. pH dependence of the uptakes of folate and methotrexate in *Xenopus laevis* oocytes expressing rPCFT/HCP1. Data represent means ± SE (*n* = 4–12). The uptakes of folate (10 nM; ●, ▲) and methotrexate (10 nM; ○, △) were evaluated at 25°C for 30 min in rPCFT/HCP1-expressing oocytes (●, ○) and water-injected control oocytes (▲, △).

Fig. 12. Effect of various compounds on folate uptake mediated by rPCFT/HCP1 expressed in *Xenopus laevis* oocytes. Data represent means ± SE (*n* = 4 or 5). The uptake of folate (10 nM) was evaluated at 37°C and pH 5.5 for 30 min in the presence or absence of a test compound in rPCFT/HCP1-expressing oocytes and water-injected control oocytes. The rPCFT/HCP1-specific uptake was estimated by subtracting the uptake in the latter from that in the former. The control value was 0.176 μl·min^{-1}·oocyte^{-1}. *Significantly different from the control at $P < 0.05$; **test compound dissolved in DMSO (0.5 or 2.0%).

were in agreement with those for carrier-mediated intestinal folate transport system evaluated by using everted sacs.

We also found that rPCFT/HCP1-mediated folate uptake is extensively reduced by pretreatment with thiol-modifying reagents of pCMBS and $HgCl_2$ to 33.8 ± 2.5 and 22.5 ± 2.1% of control (0.296 ± 0.008 $\mu l \cdot min^{-1} \cdot oocyte^{-1}$ as the uptake clearance at 10 nM), respectively, as means ± SE ($n = 4$, $P < 0.05$). This is in agreement with an earlier finding by Strum (34) in the everted sacs of the rat intestine that the pretreatment with pCMBS and iodoacetate, another thiol-modifying reagent, resulted in an inhibition of the carrier-mediated transport of methotrexate and indicates that cysteine residues, which have a thiol group, may play an important role in the function of rPCFT/HCP1.

Thus the functional characteristics of rPCFT/HCP1 were almost fully in agreement with those of carrier-mediated intestinal folate transport system, substantiating its function and role as the molecular entity of the intestinal folate transport system.

DISCUSSION

Although it has long been suggested that a pH-dependent carrier-mediated transport system is involved in intestinal absorption of folate and analogs, it was only recently that PCFT/HCP1 was identified as its possible molecular entity (19, 23). It has so far been demonstrated that the cloned hPCFT/HCP1 can specifically and efficiently transport folate and also, although with somewhat lower affinities, reduced folates and methotrexate at acidic pH with a manner characteristic to proton-coupled transport, and furthermore its loss-of-function mutation is associated with hereditary folate malabsorption, indicating its critical role in the absorption of dietary folate. In the present study using the rat model, we could further add several lines of evidence that indicate its role as the molecular entity of the intestinal folate transport system.

rPCFT/HCP1 expressed in *Xenopus laevis* oocytes was demonstrated to operate more efficiently at lower acidic pH and accept folate as a substrate with smaller K_m (higher affinity) than methotrexate (Figs. 10 and 11), indicating its characteristic as a proton-coupled folate transporter that favors folate than methotrexate as substrate. Such functional characteristics of rPCFT/HCP1 and also the profile of its inhibition by various compounds (Fig. 12) were in agreement with those of the carrier-mediated intestinal folate transport system evaluated by using everted tissue sacs (Figs. 2–5), indicating the role of rPCFT/HCP1 as its molecular entity. This proton-coupled transporter is expected to operate efficiently in vivo as well because acidic microclimate environment is known to be physiologically maintained at the intestinal surface (13). Although folates are known to be mainly in reduced forms in food, it has been suggested that they are mostly converted to the oxidized form during food processing and, after intake, digestion because reduced folates are unstable when exposed to air, heat, and acid (29). Therefore, the ability of PCFT/HCP1 to transport folate (oxidized form), as demonstrated for the rat ortholog in the present study and for the human ortholog in previous studies (19, 23), should be of physiological relevance. Since neither rPCFT/HCP1 nor the folate transport system in everted sacs were inhibited by thiamine phosphate derivatives (TPP and/or TMP), which are known as inhibitors of RFC1

(44, 45), it is most likely that these thiamine phosphate derivatives are specific to RFC1, but not to PCFT/HCP1, as inhibitor and also that the role of RFC1 in intestinal folate transport is insignificant. Furthermore, in contrast with the characteristics of rPCFT/HCP1 and the intestinal folate transport system, RFC1 reportedly operates more efficiently for the transport of reduced folates than folate (oxidized form) and at near neutral pH than acidic pH (2, 22, 26, 36). Folate binding proteins (or folate receptors) have been indicated to provide an alternative pathway of folate uptake by receptor-mediated mechanism in various tissues (33). Although the possibility that such proteins might be involved in intestinal folate uptake has also been investigated by many researchers, they are distinct from the transporters, PCFT/HCP1 and also RFC1, in having a few orders of magnitude higher affinities for folates, with half saturation concentrations in the nanomolar range, and folate binding protein (FBP) as a cloned one is absent in the intestine, as reported for the pig (37). It should also be noted that the characteristics of rPCFT/HCP1 are quite similar to those of hPCFT/HCP1 (19) and the K_m values (1 to 3 μM for folate and 3 to 6 μM for methotrexate) observed for these cloned transporters and the intestinal folate transport system in everted sacs are, for both folate and methotrexate, comparable with those reported in various intestinal preparations, 0.42 to 1.69 μM for folate (5, 12, 17, 20, 24, 28) and 0.98 to 2.8 μM for methotrexate (4, 12, 21, 25, 28, 34).

It is notable that nonsaturable (diffusive) transport was suggested to be negligible in everted tissue sacs for both folate and methotrexate from the findings that their uptakes were almost undetectable in the lowest ileum where rPCFT/HCP1 expression is almost negligible (Figs. 6 and 7) and also from kinetic analysis of their uptakes in the jejunum (Fig. 3). The complete inhibition of folate uptake by sulfasalazine also supports that (Fig. 4). Although several studies have indicated the involvement of minor diffusive transport (12, 17, 20, 21, 25, 28), it seems to be more reasonable to assume that diffusive transport is insignificant since both compounds are highly hydrophilic and fairly large in molecular weight. Compounds in this class are generally not absorbable by diffusive transport, as suggested for, e.g., β-lactam antibiotics (31).

An important finding is that the distribution of rPCFT/HCP1 along the intestinal tract is in agreement with that of the carrier-mediated folate transport system activity (Figs. 6 and 7), supporting the suggestion that rPCFT/HCP1 is its molecular entity. According to a study by Hepner et al. (10), folate absorption in the human intestine perfused in situ was high in the upper jejunum, somewhat lower in the lower jejunum, and undetectably low in the ileum, also in agreement with our observation in the rat intestine. Therefore, it is likely that hPCFT/HCP1 is highly expressed only in the upper small intestine, although it has not been examined in detail in a segmented manner (23). Although the high expression in the upper small intestine is often the case observed for nutrient transporters, the absence in the lower small intestine is not. Typically, carrier-mediated D-glucose transport can be observed in the lower small intestine in both rat and human at appreciable levels, 30 to 50% of jejunal transport (10, 42). Thus PCFT/HCP1 is markedly localized in the upper small intestine. It is as if folate were unwanted in the lower small intestine. This feature that only a limited area of the upper small intestine is available for the absorption of folates would,

however, lead to higher chances of variability in their absorption associated with alteration in intestinal transit. It would be of interest to explore the physiological meaning behind such a characteristic distribution of PCFT/HCP1.

Several members of the ATP-binding cassette (ABC) transporter family, which can facilitate the efflux of diverse organic compounds, are expressed in the apical membrane of the intestinal epithelial cells. They are presumed to play physiological roles in reducing the exposure of the body to potentially harmful compounds. Notably, BCRP is known to accept methotrexate as a substrate, and also folate and its polyglutamate conjugates (1). However, interestingly, a recent study using mice demonstrated that the expression of BCRP is gradiented in a manner opposite to that of PCFT/HCP1, lower in the upper small intestine and higher in the lower (7). This may in part explain our observation that BCRP inhibitors (diethylstilbestrol and estrone-3-sulfate) increased the jejunal uptake of neither folate nor methotrexate. It seems to be biologically designed that PCFT/HCP1 and BCRP are expressed along the intestinal tract in a coordinated manner so as for BCRP not to interfere with folate absorption. It has also been suggested that methotrexate is a substrate of MRP2, another ABC secretory transporter expressed in the intestine (14). However, its contribution in methotrexate uptake does not seem to be significant, either, as long as intestinal tissue preparation is concerned, since jejunal methotrexate uptake was not increased by estrone-3-sulfate, an MRP2 inhibitor.

Sulfasalazine was found to inhibit methotrexate transport mediated by hPCFT/HCP1 potently in our preceding study, ∼80% inhibition at its concentration of 0.2 mM (19). Consistent with that, this drug was found to inhibit folate transport mediated by rPCFT/HCP1 (Fig. 12) and also that in the everted jejunal tissue sacs by similar extents of ∼80% at its same concentration of 0.2 mM (Fig. 4). These results not only further support the suggestion that PCFT/HCP1 is responsible for the intestinal absorption of folates but also that sulfasalazine, an oral drug used for rheumatoid arthritis and ulcerative colitis, may interfere with that. The concentration of sulfasalazine (molecular weight 398.40) would be nominally ∼5 mM or higher for its clinical dose of 500 mg or larger when taken with (dissolved in) 200 ml of water, and possibly close to that in the small intestine because it is poorly absorbed (15, 16, 43). Although the solubilization status of sulfasalazine in the intestinal fluid may not be precisely predictable, it is likely that its concentration much exceeds its IC_{50} (half inhibition concentration) of ∼60 μM, which was determined in the preceding study for hPCFT/HCP1-mediated methotrexate transport (19). Thus the malabsorption of folate by inhibition of its hPCFT/HCP1-mediated transport may explain the higher risk of folate deficiency reported for patients treated with sulfasalazine (8, 9). On the other hand, indomethacin and diclofenac may least likely be involved in folate malabsorption, although they were found to inhibit rPCFT/HCP1-mediated folate transport (Figs. 4 and 12). The inhibition of folate transport by indomethacin and diclofenac was ∼70–80% at their concentration of 1 mM in everted sacs, indicating the inhibition constant (K_i) of ∼0.25 mM to 0.43 mM if competitive inhibition is assumed. This is roughly in agreement with the estimated IC_{50} (K_i under the assumption of competitive inhibition) of ∼0.2 mM or greater, which is suggested from the inhibition of ∼50% or less at their concentration of 0.2 mM, for rPCFT/HCP1-mediated transport

of folate in the present study and also for hPCFT/HCP1-mediated transport of methotrexate in our preceding study (19). Thus these drugs are consistently suggested to be less potent than sulfasalazine as inhibitors of PCFT/HCP1. Compared with the affinities of PCFT/HCP1 for folate and methotrexate, which are high with K_m values below 10 μM in both rat and human, those for these drugs seem to be only modest. Also taking into account that their typical dose (25 mg) is only about one-twentieth of the minimum dose (500 mg) of sulfasalazine and they are readily absorbed from the intestine, possibilities may be little for them to interfere with folate absorption.

In conclusion, we successfully identified that rPCFT/HCP1 is a molecule that functions as a proton-coupled folate transporter. The functional characteristics of rPCFT/HCP1 were found to be almost fully in agreement with those of carrier-mediated intestinal folate transport system, suggesting that it is the molecular entity of the intestinal folate transport system. As a finding supporting the suggestion, the distribution profile of the folate transport system activity along the intestinal tract was in agreement with that of rPCFT/HCP1 mRNA.

REFERENCES

1. **Chen ZS, Robey RW, Belinsky MG, Shchaveleva I, Ren XQ, Sugimoto Y, Ross DD, Bates SE, Kruh GD.** Transport of methotrexate, methotrexate polyglutamates, and 17β-estradiol 17-(β-D-glucuronide) by ABCG2: effects of acquired mutations at R482 on methotrexate transport. *Cancer Res* 63: 4048–4054, 2003.
2. **Chiao JH, Roy K, Tolner B, Yang CH, Sirotnak FM.** RFC-1 gene expression regulates folate absorption in mouse small intestine. *J Biol Chem* 272: 11165–11170, 1997.
3. **Chomczynski P, Sacchi N.** Single-step method of RNA isolation by acid guanidinium thiocyanate-phenol-chloroform extraction. *Anal Biochem* 162: 156–159, 1987.
4. **Chungi VS, Bourne DWA, Dittert LW.** Drug absorption VIII: kinetics of GI absorption of methotrexate. *J Pharm Sci* 67: 560–561, 1978.
5. **Chungi VS, Bourne DWA, Dittert LW.** Competitive inhibition between folic acid and methotrexate for transport carrier in the rat small intestine. *J Pharm Sci* 68: 1552–1553, 1979.
6. **Dixon KH, Lanpher BC, Chiu J, Kelley K, Cowan KH.** A novel cDNA restores reduced folate carrier activity and methotrexate sensitivity to transport deficient cells. *J Biol Chem* 269: 17–20, 1994.
7. **Enokizono J, Kusuhara H, Sugiyama Y.** Regional expression and activity of breast cancer resistance protein (bcrp/abcg2) in mouse intestine: overlapping distribution with sulfotransferases. *Drug Metab Dispos* 35: 922–928, 2007.
8. **Haagsma CJ, Blom HJ, van Riel PL, van't Hof MA, Giesendorf BA, van Oppenraaij-Emmerzaal D, van de Putte LB.** Influence of sulphasalazine, methotrexate, and the combination of both on plasma homocysteine concentrations in patients with rheumatoid arthritis. *Ann Rheum Dis* 58: 79–84, 1999.
9. **Halsted CH, Gandhi G, Tamura T.** Sulfasalazine inhibits the absorption of folates in ulcerative colitis. *N Engl J Med* 305: 1513–1517, 1981.
10. **Hepner GW, Booth CC, Cowan J, Hoffbrand AV, Mollin DL.** Absorption of crystalline folic acid in man. *Lancet* 11: 302–306, 1968.
11. **Inoue K, Fei YJ, Zhuang L, Gopal E, Miyauchi S, Ganapathy V.** Functional features and genomic organization of mouse NaCT, a sodium-coupled transporter for tricarboxylic acid cycle intermediates. *Biochem J* 378: 949–957, 2004.
12. **Itoh T, Ono K, Koido KI, Li YH, Yamada H.** Stereoselectivity of the folate transporter in rabbit small intestine: studies with amethopterin enantiomers. *Chirality* 13: 164–169, 2001.

13. **Iwatsubo T, Miyamoto Y, Sugiyama Y, Yuasa H, Iga T, Hanano M.** Effects of potential damaging agents on the microclimate-pH in the rat jejunum. *J Pharm Sci* 75: 1162–1165, 1986.

14. **Hooijberg JH, Broxterman HJ, Kool M, Assaraf YG, Peters GJ, Noordhuis P, Scheper RJ, Borst P, Pinedo HM, Jansen G.** Antifolate resistance mediated by the multidrug resistance proteins MRP1 and MRP2. *Cancer Res* 59: 2532–2535, 1999.

15. **Klotz U.** Clinical pharmacokinetics of sulphasalazine, its metabolites and other prodrugs of 5-aminosalicylic acid. *Clin Pharmacokinet* 10: 285–302, 1985.

16. **Liang E, Proudfoot J, Yazdanian M.** Mechanisms of transport and structure-permeability relationship of sulfasalazine and its analogs in Caco-2 cell monolayers. *Pharm Res* 17: 1168–1174, 2000.

17. **Mason JB, Shoda R, Haskell M, Selhub J, Rosenberg IH.** Carrier affinity as a mechanism for the pH-dependence of folate transport in the small intestine. *Biochim Biophys Acta* 1024: 331–335, 1990.

18. **Matsushima S, Maeda K, Kondo C, Hirano M, Sasaki M, Suzuki H, Sugiyama Y.** Identification of the hepatic efflux transporters of organic anions using double-transfected Madin-Darby canine kidney II cells expressing human organic anion-transporting polypeptide 1B1 (OATP1B1)/multidrug resistance-associated protein 2, OATP1B1/multidrug resistance 1, and OATP1B1/breast cancer resistance protein. *J Pharmacol Exp Ther* 314: 1059–1067, 2005.

19. **Nakai Y, Inoue K, Abe N, Hatakeyama M, Ohta K, Otagiri M, Hayashi Y, Yuasa H.** Functional characterization of human PCFT/HCP1 heterologously expressed in mammalian cells as a folate transporter. *J Pharmacol Exp Ther* 322: 469–476, 2007.

20. **Narawa T, Shimizu R, Takano S, Tsuda Y, Ono K, Yamada H, Itoh T.** Stereoselectivity of the reduced folate carrier in Caco-2 cells. *Chirality* 17: 444–449, 2005.

21. **Narawa T, Tsuda Y, Itoh T.** Chiral recognition of amethopterin enantiomers by the reduced folate carrier in Caco-2 cells. *Drug Metab Pharmacokinet* 22: 33–40, 2007.

22. **Nguyen TT, Dyer DL, Dunning DD, Rubin SA, Grant KE, Said HM.** Human intestinal folate transport: cloning, expression, and distribution of complementary RNA. *Gastroenterology* 112: 783–791, 1997.

23. **Qiu A, Jansen M, Sakaris A, Min SH, Chattopadhyay S, Tsai E, Sandoval C, Zhao R, Akabas MH, Goldman ID.** Identification of an intestinal folate transporter and the molecular basis for hereditary folate malabsorption. *Cell* 127: 917–928, 2006.

24. **Said HM, Ghishan FK, Redha R.** Folate transport by human intestinal brush-border membrane vesicles. *Am J Physiol Gastrointest Liver Physiol* 252: G229–G236, 1987.

25. **Said HM, Hollander D.** Inhibitory effect of bile salts on the enterohepatic circulation of methotrexate in the unanesthetized rat: inhibition of methotrexate intestinal absorption. *Cancer Chemother Pharmacol* 16: 121–124, 1986.

26. **Said HM, Nguyen TT, Dyer DL, Cowan KH, Rubin SA.** Intestinal folate transport: identification of a cDNA involved in folate transport and the functional expression and distribution of its mRNA. *Biochim Biophys Acta* 1281: 164–172, 1996.

27. **Schron CM, Washington C Jr, Blitzer BL.** The transmembrane pH gradient drives uphill folate transport in rabbit jejunum: direct evidence for folate/hydroxyl exchange in brush border membrane vesicles. *J Clin Invest* 76: 2030–2033, 1985.

28. **Selhub J, Rosenberg IH.** Folate transport in isolated brush border membrane vesicles from rat intestine. *J Biol Chem* 256: 4489–4493, 1981.

29. **Seyoum E, Selhub J.** Properties of food folates determined by stability and susceptibility to intestinal pteroylpolyglutamate hydrolase action. *J Nutr* 128: 1956–1960, 1998.

30. **Shayeghi M, Latunde-Dada GO, Oakhill JS, Laftah AH, Takeuchi K, Halliday N, Khan Y, Warley A, McCann FE, Hider RC, Frazer DM, Anderson GJ, Vulpe CD, Simpson RJ, McKie AT.** Identification of an intestinal heme transporter. *Cell* 122: 789–801, 2005.

31. **Sinko PJ, Amidon GL.** Characterization of the oral absorption of β-lactam antibiotics. I. Cephalosporins: determination of intrinsic membrane absorption parameters in the rat small intestine in situ. *Pharm Res* 5: 645–650, 1988.

32. **Sirotnak FM, Tolner B.** Carrier-mediated membrane transport of folates in mammalian cells. *Annu Rev Nutr* 19: 91–122, 1999.

33. **Steinberg SE.** Mechanisms of folate homeostasis. *Am J Physiol Gastrointest Liver Physiol* 246: G319–G324, 1984.

34. **Strum WB.** A pH-dependent, carrier-mediated transport system for the folate analog, amethopterin, in rat jejunum. *J Pharmacol Exp Ther* 203: 640–645, 1977.

35. **Sugimoto Y, Tsukahara S, Imai Y, Sugimoto Y, Ueda K, Tsuruo T.** Reversal of breast cancer resistance protein-mediated drug resistance by estrogen antagonists and agonists. *Mol Cancer Ther* 2: 105–112, 2003.

36. **Villanueva JA, Devlin AM, Halsted CH.** Reduced folate carrier: tissue distribution and effects of chronic ethanol intake in the micropig. *Alcohol Clin Exp Res* 25: 415–420, 2001.

37. **Villanueva J, Ling EH, Chandler CJ, Halsted CH.** Membrane and tissue distribution of folate binding protein in pig. *Am J Physiol Regul Integr Comp Physiol* 275: R1503–R1510, 1998.

38. **Wong MH, Oelkers P, Craddock AL, Dawson PA.** Expression cloning and characterization of the hamster ileal sodium-dependent bile acid transporter. *J Biol Chem* 269: 1340–1347, 1994.

39. **Williams FM, Murray RC, Underhill TM, Flintoff WF.** Isolation of a hamster cDNA clone coding for a function involved in methotrexate uptake. *J Biol Chem* 269: 5810–5816, 1994.

40. **Yuasa H, Matsuhisa E, Watanabe J.** Intestinal brush border transport mechanism of 5-fluorouracil in rats. *Biol Pharm Bull* 19: 94–99, 1996.

41. **Yuasa H, Miyamoto Y, Iga T, Hanano M.** Determination of kinetic parameters of a carrier-mediated transport in the perfused intestine by two-dimensional laminar flow model: effects of the unstirred water layer. *Biochim Biophys Acta* 856: 219–230, 1986.

42. **Yuasa H, Miyamoto Y, Iga T, Hanano M, Watanabe J.** Variation in D-glucose uptake along the intestinal tract. *J Pharmacobio-Dyn* 10: 452–455, 1987.

43. **Zaher H, Khan AA, Palandra J, Brayman TG, Yu L, Ware JA.** Breast cancer resistance protein (bcrp/abcg2) is a major determinant of sulfasalazine absorption and elimination in the mouse. *Mol Pharm* 3: 55–61, 2006.

44. **Zhao R, Gao F, Goldman ID.** Reduced folate carrier transports thiamine monophosphate: an alternative route for thiamine delivery into mammalian cells. *Am J Physiol Cell Physiol* 282: C1512–C1517, 2002.

45. **Zhao R, Gao F, Wang Y, Diaz GA, Gelb BD, Goldman ID.** Impact of the reduced folate carrier on the accumulation of active thiamin metabolites in murine leukemia cells. *J Biol Chem* 276: 1114–1118, 2001.

46. **Zimmerman J, Selhub J, Rosenberg IH.** Role of sodium ion in transport of folic acid in the small intestine. *Am J Physiol Gastrointest Liver Physiol* 251: G218–G222, 1986.